All Sciences Proceedings
http://as-proceeding.com/

1st International Conference on Pioneer and Innovative Studies
June 5-7, 2023 : Konya, Turkey

© 2023 Published by All Sciences Proceedings

ICPIS
https://as-proceeding.com/index.php/icpis

Design Process and Flow Field Analysis of a Double Divergent Supersonic Nozzle: Enhancing Efficiency and Performance

Hakim KBAB*, Sidali HAIF, Omar ABADA

Blida 1 University, Laboratory of Aeronautical Sciences, Institute of Aeronautics and Spatial Studies, P.O. 270, Soumaa Road, Blida, Algeria

**(K71.hakim@gmail.com) Email of the corresponding author*

Abstract – The dual bell nozzle concept's primary goal is to increase performance through the idea of self-adaptation for two operating regimes without mechanical activation. The dual bell nozzle type known as the planar double divergent nozzle (DDN) has a rectangular cross section. In this study we propose a numerical method for the design of the nozzle profile with double planar divergent. The design of the double divergent nozzle is carried out in two parts. The first divergent is a contour of a two-dimensional supersonic nozzle with a sharp-edged throat that gives uniform parallel flow at the exit. The method of characteristic applied to the two-dimensional isentropic flow of an ideal gas was used for the design of a supersonic planar nozzle. The contour of the second divergent (nozzle extension) is a polynomial. This is achieved using the direct method of characteristics. A numerical analysis of a double divergent nozzle, and a planar nozzle with the same area ratio and the same length using ANSYS-Fluent software. The analysis's findings indicated that the double divergent nozzle had a weight decrease of 0.61%. The thrust increase is estimated at 3.88% in the low-altitude operating mode for the double divergent nozzle.

Keywords – Dual Bell Nozzle, Double Divergent Nozzle, ANSYS-Fluent, FORTRAN, Method of Characteristics.

I. INTRODUCTION

Dual bell nozzles have been considered to maximize efficiency at high altitudes while avoiding dangerous lateral loads at low altitudes. A dual bell nozzle consists of two different contours between the throat and the exit. It is composed of a base contour separated from the extension contour by an inflection on the wall [1]. Under sea level conditions, the flow separates at the inflection point of the contour in a controlled and symmetrical manner, and the generation of lateral load continues to decrease as thrust increases due to the low surface area ratio. During flight, the ambient pressure decreases, leading to an increase in NPR (Nozzle Pressure Ratio). At a certain altitude, the transition NPR is reached, and the separation point leaves the contour inflection and rapidly moves towards the nozzle exit. Thrust improves due to the larger surface area ratio. In 1949, Cowles and Foster first introduced the concept of a dual bell nozzle, and the design was patented by Rocketdyne in the 1960s [2, 3]. As the capabilities of CFD have evolved over time, research activities have intensified in the 1990s. The first numerical analysis of dual bell nozzles was conducted by Goel and Jensen, and it was published in 1995 [4]. Throughout the 2000s, numerous experimental projects and various numerical studies on dual bell nozzles were conducted in Europe and the United States [5]. Modern studies focus on optimizing specific design variables of dual bell nozzles, such as the ideal contour and relative length of the extension section. Thanks to the wall inflection in the nozzle, it allows for altitude adaptability. Controlled and symmetrical flow separation occurs at the wall inflection point at low altitudes, resulting in a less efficient expansion ratio. The flow inside the nozzle remains attached to the wall at higher altitudes until the full geometric expansion ratio is utilized.

Improved vacuum performance is achieved due to the increased expansion ratio [6]. However, performance losses are induced in dual bell nozzles. The main advantages of this nozzle lie in its ability to control flow separation and its simple design. While other altitude compensation nozzle concepts are limited by mechanical complexity, cooling difficulties, weight, and cost, the double-curved nozzle offers an exceptional combination of simplicity, lightweight construction, performance, ease of use, and cooling [5]. Kbab et al. [7] designed the profile of a dual bell nozzle and studied the flow behavior using the method of characteristics. Genin et al. [8] tested a planar dual bell nozzle model under various flow conditions (cold flow and hot flow). Analysis of the shock in the contour inflection region provided insight into the shape and position of the separation front. At sea level, the numerical and experimental results were in good agreement, and for higher NPR values, the calculated separation position was further upstream compared to the actual position (as determined by experimentation). Verma et al. [9] conducted an experimental study to investigate the effect of Reynolds number on the transition behavior in the dual bell nozzle by conducting tests inside a high-altitude simulation chamber. Verma et al. [10] then performed experiments to study the dependence between transition behavior and fluctuations in ambient pressure inside a dual bell nozzle. Toufik et al. [11] studied the design of dual bell nozzles and evaluated several wall and performance parameters using the method of characteristics. Davis et al. [3] developed the contour design procedure for the dual bell nozzle and used it to analyze the nozzle that could be installed on a nano-satellite launcher. Genin et al. [12] conducted numerical and experimental studies to optimize the transitional behavior by varying extension geometries.

The dual bell nozzle type known as the double divergent nozzle (DDN) has a rectangular cross section. In this study we propose a numerical method for the design and numerical analysis of the nozzle profile with double planar divergent using commercial ANSYS-Fluent software. The flow pattern and thrust are studied for several pressure ratios.

II. CONCEPTION METHOD OF THE DOUBLE DIVERGENT NOZZLE

This section is intended to describe the method used to design the double divergent nozzle. The design of the double divergent nozzle is carried out in two parts:

A. *Design of the first divergent base*

The first divergent is a contour of a two-dimensional supersonic nozzle with a sharp-edged throat that gives uniform parallel flow at the exit. The method of characteristic applied to the two-dimensional isentropic flow of an ideal gas was used for the design of a supersonic planar nozzle. A sketch of a typical nozzle designed in this manner is shown in Fig. 1.

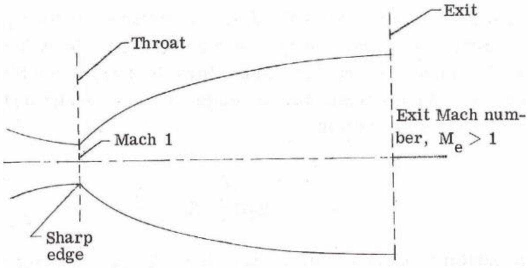

Fig. 1 Sharp-edged-throat supersonic nozzle [13].

The nomenclature for the nozzle is given in Fig. 2.

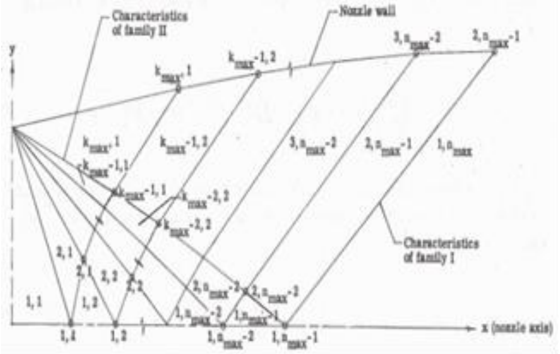

Fig. 2 Nomenclature and wave diagram for supersonic nozzle with sharp-edged throat [13].

Each small region is denoted by two index variables k and n, where k is a variable index for the characteristics of family II and n is a variable index for the characteristics of family I.

The equations and calculation procedures required to design the nozzle contour are as follows:

$$x_{k,n} = \frac{\left(y_{k+1,n+1} - m_{II} x_{k+1,n-1}\right) - \left(y_{k-1,n} - m_I x_{k-1,n}\right)}{m_I - m_{II}} \tag{1}$$

$$y_{k,n} = y_{k-1,n} + m_I \left(k_{k,n} - x_{k-1,n}\right) \tag{2}$$

$$m_I = \tan\left(\frac{u_{k,n} + u_{k-1,n+1}}{2} + \frac{\varphi_k + \varphi_{k-1}}{2}\right) \tag{3}$$

$$m_{II} = -\tan\left(\frac{u_{k,n} + u_{k+1,n}}{2} - \frac{\varphi_k + \varphi_{k+1}}{2}\right) \tag{4}$$

m_I : represent the slope for characteristics of family I

m_{II} : slope for characteristics of family II

$$u_{k,n} = \arcsin\left(\frac{1}{M_{k,n}}\right) \tag{5}$$

$$\varphi_k = (k-1)\Delta\nu \tag{6}$$

u : Mach angle
φ : Flow angle

$$M_{k,n} = \sqrt{\frac{\left(\frac{2}{\gamma+1}\right) M^{*2}_{k,n}}{1 - \left(\frac{\gamma-1}{\gamma+1}\right) M^{*2}_{k,n}}} \tag{7}$$

The waves of family II extend beyond the region where the two families exist and cut the contour of the nozzle, which is shaped so as to cancel these waves. For the nozzle contour points, we solve the following set of equations: equation (1), (2) and $k = k_{\max}$. For more details, see Reference [13].

B. *Design of the second divergent*

The contour of the nozzle extension (second bell) is designed to give a constant wall Mach number M_2. This is done by applying the characteristics method to the Prandtl-Meyer expansion around junction point J with equal intensity $\frac{M_2}{M_1}$(see Fig. 3) for the inviscid fluid hypothesis.

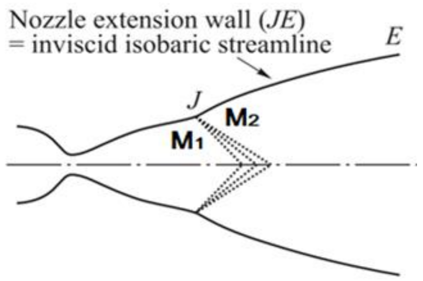

Fig. 3 Centered expansion at junction J [14]

III. PROGRAM RESULTS

Figure 4 represents the double divergent nozzle profile with its mesh (in red) obtained by our FORTRAN program.

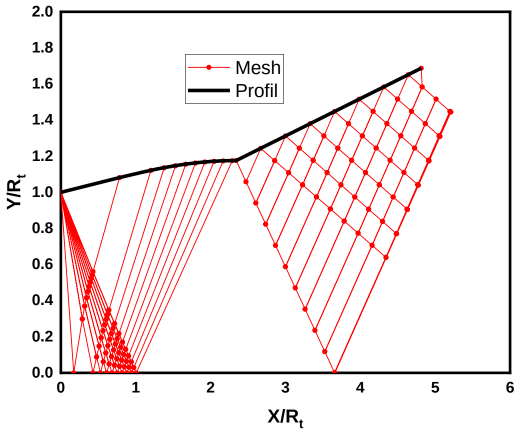

Fig. 4 The obtained double divergent nozzle contour.

A double divergent nozzle with an exit Mach number for the first divergent (divergent base) equal to 1.5.

Figures 5 represent the evolution of the Mach number along the wall of the double divergent nozzle. There is an increase in the wall Mach value of up to 1.9 for double divergent nozzle and stability at this value.

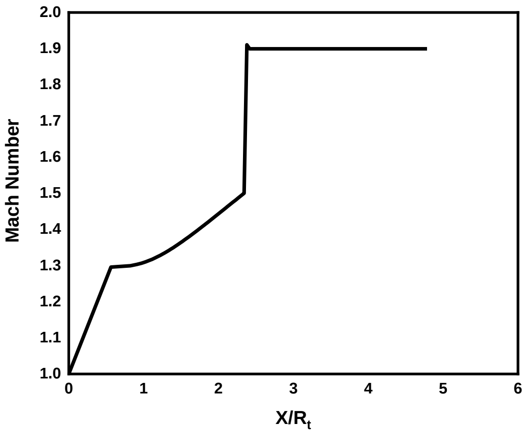

Fig. 5 Mach calculated by MOC for Double Divergent Nozzle.

The wall pressure ratio (wall pressure/total pressure) distribution on double divergent nozzle calculated by MOC is presented in Fig. 6. We note that there are two phases of wall pressure reduction. In the first phase we observe a low wall pressure of 0.13 for double divergent nozzle. In the second phase, we notice that there is a stability in the wall pressure ratio at 0.13.

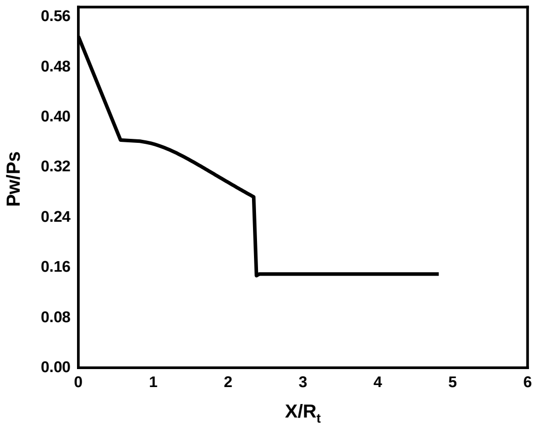

Fig. 6 Wall pressure calculated by MOC for double divergent nozzle.

IV. NUMERICAL SIMULATIONS

A numerical analysis of a double divergent nozzle, and a planar nozzle with the same area ratio and the same length using ANSYS-Fluent software.

A double divergent nozzle with an exit Mach number for the first divergent (divergent base) equal to 2.5 and a second divergent (extension) extended to achieve the same length and same section ratio of the planar nozzle (see Fig. 7).

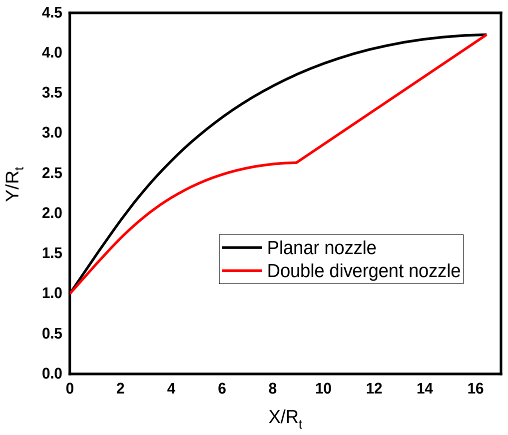

Fig. 7 Profile nozzles

In the case of the double divergent nozzle, the profile of the second divergent has been determined using a polynomial curve of the first degree. Whose constants are calculated from the initial conditions.

Table 1. Thrust comparison for the two nozzles

	Planar Nozzle	**Double Divergent Nozzle**	**Weight gain%**
Area (m^2)	0.169094	0.168070	0.61

Table 1 provides a surface comparison between the double divergent nozzle and the planar nozzle. It indicates that the double divergent nozzle is approximately 0.61% lighter than the planar nozzle. This weight reduction implies potential fuel savings and suggests that the double divergent nozzle offers advantages in terms of weight efficiency. The comparison was made by calculating the respective areas of both nozzles to facilitate a meaningful comparison of their weights.

In this section, we conducted a numerical analysis on the flow through the double divergent and planar nozzles. All geometries were examined with similar boundary conditions, and a flow analysis was performed. The numerical analysis was carried out on 2D planar models using the commercial ANSYS-Fluent software. To model the turbulence, the k-ω SST model was employed. The baseline solver chosen was a double-precision density-based coupled solver with Implicit Time Integration. Spatial discretization utilized the least-square cell-based gradient, assuming linear variation of the solution, while a second-order upwind scheme was employed for interpolating pressure, momentum, turbulent kinetic energy, specific dissipation rate, and energy values. The computational analysis was conducted under steady conditions. To initiate the steady-state problem, full multigrid (FMG) initialization was applied to obtain the initial solution, and the inlet boundary conditions were specified to establish the reference value. The Sutherland equation was used to calculate the viscosity of air.

Table 2 displays the boundary condition values applied to both the double divergent nozzle and planar nozzle. To accurately replicate the physics of the problem under investigation, the total feeding pressure was maintained constant, while the ambient pressure was varied according to the following sequence: NPR=7.5 (low altitude mode, overexpansion) and NPR=40 (under-expansion). Here, NPR represents the ratio of the total feeding pressure to the ambient pressure.

Table 2. Boundary conditions values

	Double divergent nozzle and Planar nozzle
Gauge Total Pressure (Pa)	200000
Supersonic/Initial Gauge Pressure (Pa)	105656
Total Temperature (K)	330

Figures 7 to 10 below illustrate the progression of the Mach number contours of both the double divergent nozzle and planar nozzle for different values of the differential pressure ratio (NPR).

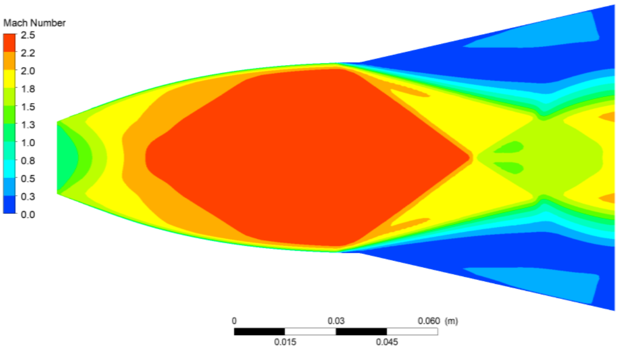

Fig. 7 Iso-Mach contour of the double divergent nozzle for NPR=7.50.

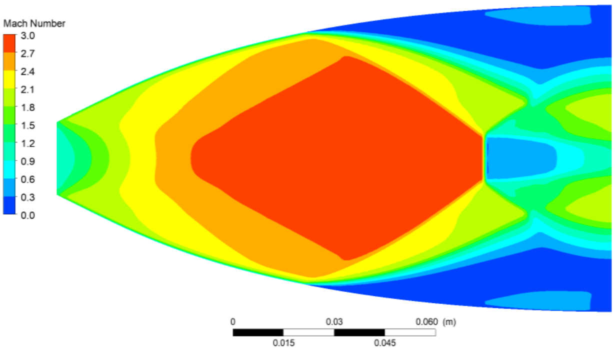

Fig. 8 Iso-Mach contour of the planar nozzle for NPR=07.50.

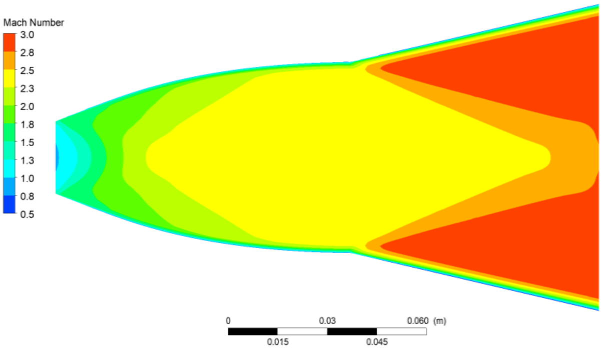

Fig. 9 Iso-Mach contour of the double divergent nozzle for NPR=40.00.

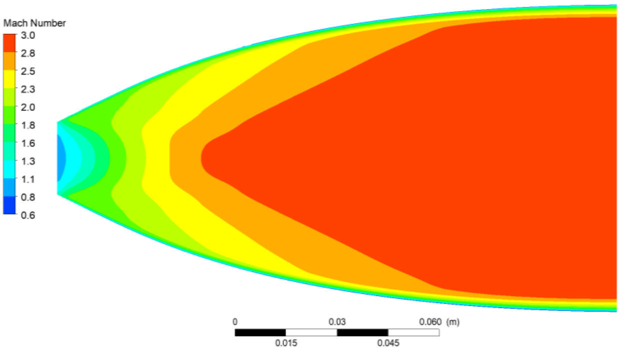

Fig. 10 Iso-Mach contour of the planar nozzle for NPR=40.00.

In the case of NPR=7.50 (low altitude mode), it can be observed that flow separation occurs in both nozzles. Specifically, in the double divergent nozzle, the flow separation takes place at the inflection point, which results in reduced side loads during low altitude operation.

Finally, for NPR=40.00 (under-expansion), there is an expansion of the flow in both nozzles. This indicates that the pressure ratio is sufficient to achieve optimal expansion.

Table 3. Thrust comparison for the two nozzles

NPR	**Planar Nozzle**	**Planar Double Divergent Nozzle**	**Thrust gain (%)**
07.50	1950.100	2025.757	3.88
40.00	2874.152	2853.195	-0.73

Table 3 displays the thrust generated by both the double divergent nozzle and the planar nozzle for NPR values of 07.50 and 40.00. It is worth noting that for NPR values of 07.50, the double divergent nozzle delivers a significantly higher thrust compared to the planar nozzle, with an approximate increase of 3.88%.

Furthermore, at NPR=40.00, the thrust produced by both the double divergent nozzle and the planar nozzle is nearly equal. This can be attributed to the fact that both nozzles have the same area ratio, resulting in comparable performance at this specific NPR.

Overall, the table provides insights into the thrust characteristics of the planar double divergent nozzle and the planar nozzle across different NPR values.

V. CONCLUSION

This research aimed to examine and compare the performance of the double divergent nozzle with the planar nozzle. The study involved conducting a numerical analysis using the ANSYS-Fluent software on both the double divergent nozzle and the planar nozzle, which had the same area ratio and length.

The analysis results revealed several findings. Firstly, the double divergent nozzle exhibited a weight reduction of 0.61% compared to the planar nozzle. Secondly, in terms of thrust, the double divergent nozzle demonstrated significant improvements. In the low-altitude operating mode, there was a thrust increase of approximately 3.88% for the double divergent nozzle.

In the low-altitude mode, it was observed that the flow separation occurred at the inflection point in the double divergent nozzle. This separation phenomenon helped reduce side loads, which is advantageous for operations at low altitudes.

Furthermore, at NPR=40.00, the thrust generated by the double divergent nozzle and the planar nozzle was nearly equal. This indicates that both nozzles performed similarly at this specific NPR value.

Overall, this research provided valuable insights into the performance characteristics of the double divergent nozzle compared to the planar nozzle, highlighting its weight reduction, thrust enhancements in specific operating modes, and flow separation benefits at low altitudes.

REFERENCES

[1] R. Stark, C. Génin, D. Schneider, and C. Fromm, C. “Ariane 5 performance optimization using dual-bell nozzle extension,” *Journal of Spacecraft and Rockets*, Vol. 53, pp. 743–750, 2016.

[2] M. Horn, and S. Fisher, Dual-bell altitude compensating nozzles. Pennsylvania State Univ., NASA Propulsion Engineering Research Center. Vol. 2, 1993.

[3] K. Davis, E. Fortner, M. Heard, H. McCallum, and H. Putzke, “Experimental and computational investigation of a dual-bell nozzle,” in Proc. *53rd AIAA Aerospace Sciences Meeting*, 2015.

[4] M. Frey, and G. Hagemann, “Critical assessment of dual-bell nozzles,” *Journal of Propulsion and Power*, Vol. 15, pp. 137–143, 1999.

[5] G. Hagemann, H. Immich, T. Van Nguyen, G. E. Dumnov, “Advanced rocket nozzles,” *Journal of Propulsion and Power*, Vol. 14, pp. 620–634, 1998.

[6] E. Martelli, F. Nasuti, and M. Onofri, “Numerical parametric analysis of dual-bell nozzle flows,” *AIAA Journal*, Vol. 45, pp. 640–650, 2007.

[7] H. Kbab, M. Sellam, T. Hamitouche, S. Bergheul, and L. Lagab, “Design and performance evaluation of a dual bell nozzle,” *Acta Astronautica*, Vol. 130, pp.52–59, 2017.

[8] C. Génin, R. Stark, O. Haidn, K. Quering, and M. Frey, “Experimental and numerical study of dual bell nozzle flow,” *Progress in Flight Physics*, Vol. 5, pp. 363–376, 2013.

[9] S. Verma, R. Stark, and O. Haidn, “Reynolds number influence on dual-bell transition phenomena*,” Journal of Propulsion and Power*, Vol. 29, pp. 602–609, 2013.

[10] S. Verma, R. Stark, and O. Haidn, “Effect of ambient pressure fluctuations on dual-bell transition behavior,” *Journal of Propulsion and Power*, Vol. 30, pp. 1192–1198, 2014.

[11] H. Toufik, H. Kbab, M. Sellam, S. Bergheul, and L. Lagab, “Design and performances of the dual-bell nozzle,” in *Proc. 2016 IEEE Aerospace Conference*, 2016.

[12] C. Genin, R. H. Stark, and D. Schneider, “Transitional behavior of dual bell nozzles: contour optimization*,” in Proc. 49th AIAA/ASME/SAE/ASEE Joint PropulsionConference*, 2013, pp. 3841.

[13] R. Micbael, and L. GOLDMAN, “Computer program for Design Of Two-Dimensional Supersonic Nozzle with Sharp-Edged Throat”, NASA TM X-1502, 1963.

[14] P. Reijasse, D. Coponet, J. M. Luyssen, V. Bar, S. Palerm, J. Oswald, and P. Kuszla, "Wall Pressure and Thrust of a Dual Bell Nozzle in a Cold Gas Facility," *Progress in Propulsion Physics*, Vol. 2, pp. 655–674, 2011.